Journal of Sound and Vibration 333 (2014) 5269–5282

Contents lists available at ScienceDirect

Journal of Sound and Vibration

journal homepage: www.elsevier.com/locate/jsvi

Multi-objective control for active vehicle suspension with wheelbase preview

Panshuo Li *, James Lam, Kie Chung Cheung

Department of Mechanical Engineering, The University of Hong Kong, Pokfulam Road, Hong Kong

ARTICLE INFO

Article history:
Received 6 September 2013
Received in revised form
2 March 2014
Accepted 12 June 2014
Handling Editor: D.J. Wagg
Available online 3 July 2014

ABSTRACT

This paper presents a multi-objective control method with wheelbase preview for active vehicle suspension. A four-degree-of-freedom half-car model with active suspension is considered in this study. H_∞ norm and generalized H_2 norm are used to improve ride quality and ensure that hard constraints are satisfied. Disturbances at the front wheel are obtained as preview information for the rear wheel. Static output-feedback is utilized in designing controllers, the solution is derived by iterative linear matrix inequality (ILMI) and cone complementarity linearization (CCL) algorithms. Simulation results confirm that multi-objective control with wheelbase preview achieves a significant improvement of ride quality (a maximum 27 percent and 60 percent improvement on vertical and angular acceleration, respectively) comparing with that of control without preview, while suspension deflections, tyre deflections and actuator forces remaining within given bounds. The extent of the improvement on the ride quality for different amount of preview information used is also illustrated.

1. Introduction

Vehicle suspension is used to provide good ride quality, good handling, maintain road holding ability and support vehicle static weight [1]. Aiming to improve ride quality and safety, many researchers have paid great attention to study different types of vehicle suspension, from passive, semi-active, to active ones. Passive suspension is simple and reliable, but its performance is limited. Semi-active suspension is better than passive suspension, but it has limited ability to meet high performance demands. Active suspension has drawn much attention in recent years because of its potential to meet tight performance requirements demanded by consumers, it can improve ride quality, and maintain good handling and road holding simultaneously.

Preview control was first proposed by Bender [2], who considered knowledge of road surface that could further improve suspension performance. This scheme allows the controller to prepare for the incoming disturbances. Comparing with pure feedback control, it utilizes preview information and promises significant improvement in performance. Similar results had also been reported by Tomizuka from the viewpoint of discrete optimal control in [3], and a preview controller which is suited for practical use had been derived. Until now, there are two common ways to obtain preview information. One is to install a sensor in front of the front wheel, which is called "look-ahead preview," the other is to use the front wheel disturbance as preview information for the rear wheel, called "wheelbase preview." In the look-ahead preview, preview

* Corresponding author.
E-mail addresses: panshuoli812@gmail.com (P. Li), james.lam@hku.hk (J. Lam), kccheung@hku.hk (K.C. Cheung).

http://dx.doi.org/10.1016/j.jsv.2014.06.017
0022-460X/

information is obtained by a laser sensor, and available for both front and rear wheels. Many studies [4–14] are based on this method. Hac [4] derived the state-feedback control gain with a quarter-car model and showed that the suspension performance could be improved by using preview information. Marzbanrad et al. [5,6] developed Hac's result to half-car and full-car models, good performances had also been reported. Preview control with an estimation scheme was investigated in [7]. Thompson and Pearce [8] developed a program which could be used to calculate the performance index and control gains for an suspension with the preview scheme. The influence of preview uncertainty on the performance had been studied in [9], the results showed that tyre deformation was the most sensitive to preview noise, while the suspension deflection was less affected. Elmadany et al. [10] considered the application of stochastic optimal control to design an active suspension with preview under the integral constraint. A spectral decomposition method was applied to compute the RMS value of control forces, suspension deflections and tyre deflections in a suspension system with preview in [11]. By using the preview information, Youn and Hac [12] derived the control law with calculus of variations. Preview control had also been used in the semi-active suspension design. A semi-active control method had been proposed to the suspension system with hysteretic nonlinear suspension spring in [13]. H_∞ control with preview had been proposed to the suspension system with magnetorheological dampers in [14]. However, apart from the high cost of a laser sensor, look-ahead preview has a natural disadvantage that preview information is not reliable at times. For example, it might not recognize a pothole just because it is full of rain water, or regard a soft sponge as a hard bump. Incorrect preview information will lead to a wrong decision from the controller, which will adversely affect the suspension performance. Referring to wheelbase preview, the preview information is more reliable, since it directly comes from system responses under disturbance at the front wheel. Many researchers have contributed to this method. Yu [15,16] used the Padé approach to estimate the disturbance at the rear wheel real-time, and designed a controller by optimization. Park and Roh [17] treated this method in discrete-time and used the state-feedback controller with the state being estimated by a Kalman–Bucy filter. Xie et al. [18] proposed a PID controller combining with a nonlinear differentiator to deal with this problem. Zhang and Zhang [19] applied a preview control to a limited bandwidth active suspension, both look-ahead and wheelbase preview information are utilized.

Various approaches have been proposed in suspension design. The semi-active and active controls of suspension have received a lot of attention. For example, the semi-active control has been designed using MR dampers in [20–25]. On the other hand, the active control can further improve vibration control performance on vehicles. Successful results have been reported using a variety of control strategies, such as fuzzy control [26–28], H_∞ control [29–31], adaptive control [32,33]. In preview control schemes, almost all researchers [4–7,10,11,17,19] employed Linear quadratic-based optimization approaches in quarter-car, half-car and full-car models. This method needs a compromise between conflicting performance requirements, the designer should make a trade-off among ride quality, good handling, road holding and actuator saturation. The design is formulated as a single-objective strategy. On the other hand, the multi-objective control has been utilized in active suspension in [30,34–37]. The results showed the multi-objective control to achieve better performance than linear quadratic-based optimization. In [38,39], Akbari applied multi-objective control with look-ahead preview in a quarter-car model. It was verified with experiment that the results are more effective when compared with the look-ahead preview with the linear quadratic Gaussian approach.

Motivated by the above discussion, in this paper, we present a multi-objective control for the active suspension system with wheelbase preview. The differences between this paper and the previous works are identified as follows: (1) multi-objective control has combined with wheelbase preview strategy; (2) static output-feedback has been utilized to design the controller, because it is considerably easier to be realized in practice and is more amenable to analyze the characteristics of the preview control with different preview sampling periods; (3) the effects of different numbers of preview information on the suspension performance have been studied. A half-car suspension model is considered here because of the wheelbase preview scheme. The H_∞ norm is used to measure the ride quality and generalized H_2 norm is used to deal with the hard constraints on the peak amplitudes of some variables. The rest of this paper is organized as follows. Section 2 gives the half-car suspension model used for subsequent development. An augmented system with wheelbase preview information is established in Section 3. Based on the augmented system, a discrete-time multi-objective static output-feedback controller is derived via iterative linear matrix inequality (ILMI) and cone complementarity linearization (CCL) algorithms in Section 4. In Section 5, simulation results and the corresponding analyses are presented. Conclusions are given in Section 6.

Notation: Throughout the paper, the superscript T refers to matrix transposition; $\mathbf{I}_n$ represents $n \times n$ identity matrix and $\mathbf{0}_{n\times m}$ represents $n \times m$ zero matrix; $\mathbb{R}^{n\times m}$ stands for the set of $n \times m$ real matrix; $\mathbb{E}(\cdot)$ denotes the expectation operator. l_2 denotes the space of square summable vectors; $|\cdot|$ denotes the absolute value and $\|\cdot\|$ denotes the Euclidean norm of a vector and its induced norm of a matrix; $\mathbb{N}_0$ denotes the set of non-negative integers. $\mathbf{P} > \mathbf{0}$ means $\mathbf{P}$ is a real symmetric and positive definite matrix; the notation $*$ represents a term that is induced by symmetry; $\dim(\cdot)$ stands for the dimension of a matrix; $\mathrm{tr}(\cdot)$ denotes the trace of a matrix.

2. Half-car suspension model

A half-car model with four degrees of freedom is given in Fig. 1. This model contains heave and pitch modes of the sprung mass. Assume that the pitch angle is small, and the characteristics of the suspension elements are linear, the equations of motion can be given as

$$M\ddot{z}_c = f_f + f_r,$$

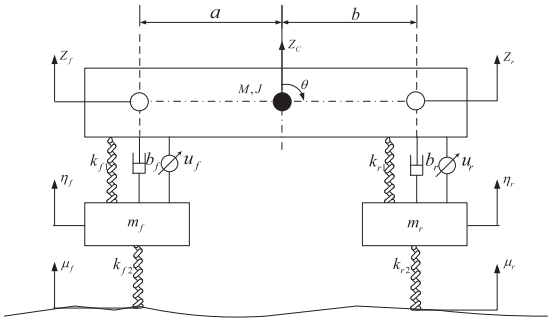

Fig. 1. Half-car model.

$$\begin{aligned} J\ddot{\theta} &= af_f - bf_r, \\ m_f\ddot{z}_1 &= -k_{f2}(\eta_f - \mu_f) - f_f, \\ m_r\ddot{z}_2 &= -k_{r2}(\eta_r - \mu_r) - f_r, \end{aligned} \tag{1}$$

where

$$f_f = k_{f1}(\eta_f - z_c - a\theta) + b_f(\dot{\eta}_f - \dot{z}_c - a\dot{\theta}) + u_f,$$

$$f_r = k_{r1}(\eta_r - z_c + b\theta) + b_r(\dot{\eta}_r - \dot{z}_c + b\dot{\theta}) + u_r,$$

where a and b denote the horizontal distances from the center of mass to the front wheel and rear wheels, respectively. M and J are the sprung mass and its mass moment of inertia, m_f and m_r are the front and rear unsprung masses, respectively, and u_f and u_r are the control forces. Parameters $k_{f\ 1}$, $k_{r\ 1}$ and b_f, b_r denote, respectively, the stiffnesses and damping coefficients of the passive suspension elements for the front and rear assemblies. Similarly, $k_{f\ 2}$ and $k_{r\ 2}$ denote the front and rear tyre stiffnesses. Tyre damping is ignored in this model, because it is always much smaller than the suspension damping.

It is convenient to choose the state vector as

$$\mathbf{x} = [x_1\ x_2\ x_3\ x_4\ x_5\ x_6\ x_7\ x_8]^T,$$

where

$$\begin{aligned} x_1 = z_c + a\theta, \quad x_2 = z_c - b\theta, \quad x_3 = \eta_f, \quad x_4 = \eta_r, \\ x_5 = \dot{z}_c + a\dot{\theta}, \quad x_6 = \dot{z}_c - b\dot{\theta}, \\ x_7 = \dot{\eta}_f, \quad x_8 = \dot{\eta}_r. \end{aligned} \tag{2}$$

Introducing the control input, road input as follows:

$$\mathbf{u} = \begin{bmatrix} u_f \\ u_r \end{bmatrix}, \quad \mathbf{w} = \begin{bmatrix} w_f \\ w_r \end{bmatrix} = \begin{bmatrix} \mu_f \\ \mu_r \end{bmatrix}, \tag{3}$$

where w_r is time-delay of w_f, that is, $w_r(t) = w_f(t-\tau)$, $\tau = (a+b)/v$, and v is the vehicle forward velocity (m/s).

Then the governing equations can be presented in the following state-space form and $\mathbf{y}$ is the measurement output:

$$\begin{aligned} \dot{\mathbf{x}}(t) &= \mathbf{A}\mathbf{x}(t) + \mathbf{B}\mathbf{u}(t) + \mathbf{D}\mathbf{w}(t), \\ \mathbf{y}(t) &= \mathbf{C}_y\mathbf{x}(t), \end{aligned} \tag{4}$$

where

$$\mathbf{A} = \begin{bmatrix} \mathbf{0}_{4\times4} & \mathbf{I}_4 \\ \mathcal{A} & \end{bmatrix},$$

$$\mathcal{A} = \begin{bmatrix} -a_1k_{f1} & -a_2k_{r1} & a_1k_{f1} & a_2k_{r1} & -a_1b_f & -a_2b_r & a_1b_f & a_2b_r \\ -a_2k_{f2} & -a_3k_{r1} & a_2k_{f1} & a_3k_{r1} & -a_2b_f & -a_3b_r & a_2b_f & a_2b_r \\ \frac{k_{f1}}{m_f} & 0 & -\frac{k_{f1}+k_{f2}}{m_f} & 0 & \frac{b_f}{m_f} & 0 & -\frac{b_f}{m_f} & 0 \\ 0 & \frac{k_{r1}}{m_r} & 0 & -\frac{k_{r1}+k_{r2}}{m_r} & 0 & \frac{b_r}{m_r} & 0 & -\frac{b_r}{m_r} \end{bmatrix},$$

$$\mathbf{B} = \begin{bmatrix} \mathbf{0}_{4\times1} & \mathbf{0}_{4\times1} \\ a_1 & a_2 \\ a_2 & a_3 \\ -\frac{1}{m_f} & 0 \\ 0 & -\frac{1}{m_r} \end{bmatrix},$$

$$\mathbf{D}=\begin{bmatrix}\mathbf{0}_{6\times1} & \mathbf{0}_{6\times1}\\ \frac{k_{f2}}{m_f} & 0\\ 0 & \frac{k_{r2}}{m_r}\end{bmatrix},$$

$$\mathbf{C}_y=\mathbf{I}_8,$$

with

$$a_1=\frac{1}{M}+\frac{a^2}{J},\quad a_2=\frac{1}{M}-\frac{ab}{J},\quad a_3=\frac{1}{M}+\frac{b^2}{J}.$$

When designing an active vehicle suspension, the following aspects are focused:

(1) *Ride quality*: A well-designed vehicle suspension provides isolation by reducing forces transmitted from vehicle axle to vehicle body [1]. The accelerations of the sprung mass are used as the indicators. Therefore, in control design, one of the objectives is to minimize $\ddot{z}_c$, and $\ddot{\theta}$ under disturbances.

(2) *Suspension deflection limit*: Vehicle suspension should support the vehicle static weight. Suspension deflection has to be considered to avoid excessive suspension bottoming, which may lead to structural damage. The suspension stroke should be confined to a prescribed range, that is,

$$\begin{aligned}|z_f-\eta_f|&\le z_{f\max},\\ |z_r-\eta_r|&\le z_{r\max},\end{aligned}\tag{5}$$

where $z_{f\max}$ and $z_{r\max}$ are the maximum suspension deflections at the front and rear, respectively.

(3) *Road holding*: It calls for a firm uninterrupted contact between the wheels and the road under disturbances. The dynamic tyre load should not exceed the static one [40], that is

$$\begin{aligned}k_{f2}\left(\eta_f-\mu_f\right)&<9.8\left(\frac{bM}{a+b}+m_f\right),\\ k_{r2}\left(\eta_r-\mu_r\right)&<9.8\left(\frac{aM}{a+b}+m_r\right).\end{aligned}\tag{6}$$

(4) *Actuator saturation*: Considering the limited actuating power, the active control force should not exceed a certain limit, that is,

$$\begin{aligned}|u_f|&\le u_{f\max},\\ |u_r|&\le u_{r\max},\end{aligned}\tag{7}$$

where $u_{f\max}$ and $u_{r\max}$ are the maximum control inputs for the front and rear wheels, respectively.

It can be seen that the accelerations of the sprung mass should be minimized to provide good ride quality, while the latter three limitations are hard constraints which need to be satisfied simultaneously. According to the different objectives, the following output variables are defined:

$$\mathbf{z}_1(t)=\begin{bmatrix}\ddot{z}_c & \ddot{\theta}\end{bmatrix}^T,$$

$$\mathbf{z}_2(t)=\begin{bmatrix}\frac{z_f-\eta_f}{z_{f\max}} & \frac{z_r-\eta_r}{z_{r\max}} & \frac{k_{f2}(\eta_f-\mu_f)}{9.8(\frac{bM}{a+b}+m_f)} & \frac{k_{r2}(\eta_r-\mu_r)}{9.8(\frac{aM}{a+b}+m_r)} & \frac{u_f}{u_{f\max}} & \frac{u_r}{u_{r\max}}\end{bmatrix}^T.\tag{8}$$

Notice that the quantity $\mathbf{z}_2$ has been normalized. By using state-space description, $\mathbf{z}$ can be rewritten as

$$\begin{aligned}\mathbf{z}_1(t)&=\mathbf{C}_1\mathbf{x}(t)+\mathbf{D}_1\mathbf{u}(t)+\mathbf{D}_{w1}\mathbf{w}(t),\\ \mathbf{z}_2(t)&=\mathbf{C}_2\mathbf{x}(t)+\mathbf{D}_2\mathbf{u}(t)+\mathbf{D}_{w2}\mathbf{w}(t),\end{aligned}\tag{9}$$

where

$$\mathbf{C}_1=\begin{bmatrix}-\frac{k_{f1}}{M} & -\frac{k_{r1}}{M} & \frac{k_{f1}}{M} & \frac{k_{r1}}{M} & -\frac{b_f}{M} & -\frac{b_r}{M} & \frac{b_f}{M} & \frac{b_r}{M}\\ -a\frac{k_{f1}}{J} & b\frac{k_{r1}}{J} & -a\frac{k_{f1}}{J} & -b\frac{k_{r1}}{J} & -a\frac{b_f}{J} & b\frac{b_r}{J} & a\frac{b_f}{J} & -b\frac{b_r}{J}\end{bmatrix},$$

$$\mathbf{D}_1=\begin{bmatrix}\frac{1}{M} & \frac{1}{M}\\ \frac{a}{J} & -\frac{b}{J}\end{bmatrix},\quad \mathbf{D}_{w1}=\mathbf{0}_{2\times2},$$

$$\mathbf{C}_2=\begin{bmatrix} \frac{1}{z_{f\max}} & 0 & -\frac{1}{z_{f\max}} & 0 & \mathbf{0}_{1\times4} \\ 0 & \frac{1}{z_{r\max}} & 0 & -\frac{1}{z_{r\max}} & \mathbf{0}_{1\times4} \\ 0 & 0 & \frac{k_{f2}}{9.8\left(\frac{bM}{a+b}+m_f\right)} & 0 & \mathbf{0}_{1\times4} \\ 0 & 0 & 0 & \frac{k_{r2}}{9.8\left(\frac{aM}{a+b}+m_r\right)} & \mathbf{0}_{1\times4} \\ \mathbf{0}_{2\times1} & \mathbf{0}_{2\times1} & \mathbf{0}_{2\times1} & \mathbf{0}_{2\times1} & \mathbf{0}_{2\times4} \end{bmatrix},$$

$$\mathbf{D}_2=\begin{bmatrix} \mathbf{0}_{4\times1} & \mathbf{0}_{4\times1} \\ \frac{1}{u_{f\max}} & 0 \\ 0 & \frac{1}{u_{r\max}} \end{bmatrix},\quad \mathbf{D}_{w2}=\begin{bmatrix} \mathbf{0}_{2\times1} & \mathbf{0}_{2\times1} \\ -\frac{k_{f2}}{9.8\left(\frac{bM}{a+b}+m_f\right)} & 0 \\ 0 & -\frac{k_{r2}}{9.8\left(\frac{aM}{a+b}+m_f\right)} \\ \mathbf{0}_{2\times1} & \mathbf{0}_{2\times1} \end{bmatrix}.$$

With system sampling period T_s, a discrete-time representation of the half-car model can be obtained as

$$\begin{aligned} \mathbf{x}(k+1)&=\mathbf{G}\mathbf{x}(k)+\mathbf{H}\mathbf{u}(k)+\mathbf{F}\mathbf{w}(k),\\ \mathbf{z}_1(k)&=\mathbf{C}_1\mathbf{x}(k)+\mathbf{D}_1\mathbf{u}(k)+\mathbf{D}_{w1}\mathbf{w}(k),\\ \mathbf{z}_2(k)&=\mathbf{C}_2\mathbf{x}(k)+\mathbf{D}_2\mathbf{u}(k)+\mathbf{D}_{w2}\mathbf{w}(k),\\ \mathbf{y}(k)&=\mathbf{C}_y\mathbf{x}(k), \end{aligned} \tag{10}$$

where $\mathbf{G},\mathbf{H},\mathbf{F}$ are the discrete-time equivalents of continuous-time system matrices $\mathbf{A},\mathbf{B},\mathbf{D}$, respectively, obtained by step-invariant discretization.

3. Augmented system with wheelbase preview information

Let $\mathbf{x}_a(k)$ denote the vector which represents all the preview information for the rear wheel,

$$\mathbf{x}_a(k)=\begin{bmatrix} w_f(k-N_a) \\ w_f(k-N_a+1) \\ \vdots \\ w_f(k-1) \\ w_f(k) \end{bmatrix},$$

in which $N_a\in\mathbb{N}_0$ is the integral part of τ/T_s.

The road surface elevation process $w_f(t)$ at the front wheel can be modeled as [17,41]:

$$\dot{w}_f+\alpha v w_f=\xi \tag{11}$$

where α is a constant related to type of road surface, ξ is a Gaussian white noise process with

$$\mathbb{E}[\xi(t_1)\xi(t_2)^T]=2\alpha v\sigma^2\delta(t_1-t_2) \tag{12}$$

where σ is the standard deviation of road unevenness and $\delta(t)$ is the Dirac delta. In the current work, it is assumed that the vehicle velocity and the road profile are not varying with respect to time. However, in practice, these parameters are variables. For interested readers, there are some works about the road identification techniques, see [20,24,42].

The discrete-time representation of the disturbances at the front and rear wheels is thus given by

$$\begin{aligned} w_f(k+1)&=G_w w_f(k)+\phi(k),\\ w_r(k)&=w_f(k-N_a), \end{aligned} \tag{13}$$

where $G_w=e^{-\alpha vT_s}$ and $\phi(k)$ can be given as a stochastic integral [43,44]:

$$\phi(k)=\int_{kT_s}^{(k+1)T_s} e^{-\alpha v[(k+1)T_s-s]}\,\mathrm{d}W(s) \tag{14}$$

where $W(s)$ is the Wiener process with $\mathbb{E}(\mathrm{d}W^2)=2\alpha v\sigma^2\,\mathrm{d}t$, and $\phi(k)$ has the following statistical properties:

$$\begin{aligned} \mathbb{E}(\phi(k))&=0\\ \mathbb{E}(|\phi(k)|^2)&=2\alpha v\sigma^2\mathbb{E}\left(\int_{kT_s}^{(k+1)T_s}|e^{-\alpha v[(k+1)T_s-s]}|^2\,\mathrm{d}s\right)\\ &=\sigma^2(1-e^{-2\alpha vT_s}) \end{aligned} \tag{15}$$

Then the state-space equation of the augmented vector x_a can be easily obtained as

$$\mathbf{x}_a(k+1)=\mathbf{G}_a\mathbf{x}_a(k)+\mathbf{F}_a\psi(k), \tag{16}$$

where

$$\mathbf{G}_a=\begin{bmatrix}0&1&0&0&\cdots&0\\0&0&1&0&\cdots&0\\\vdots&\vdots&&\ddots&&\vdots\\0&0&0&\cdots&1&0\\0&0&0&\cdots&0&1\\0&0&0&\cdots&0&G_w\end{bmatrix},\quad \mathbf{F}_a=\begin{bmatrix}0\\\vdots\\0\\\sqrt{\sigma^2(1-e^{-2\alpha vT_s})}\end{bmatrix},$$

and $\mathbf{G}_a\in\mathbb{R}^{(N_a+1)\times(N_a+1)}$, $\mathbf{F}_a\in\mathbb{R}^{(N_a+1)\times 1}$. The effective input ψ is a unit variance white noise sequence.

Let us denote the preview sampling period, used for collecting preview information from $\mathbf{x}_a$, as T_p. $\mathbf{y}_a(k)$ denotes the measurement output vector which represents the available preview information for the rear wheel with T_p as the preview sampling period. The preview sampling period is an integral multiple of the system sampling period, that is, $T_p=\ell T_s, \ell=1,2,\ldots$. Then $\mathbf{y}_a(k)$ can be written as

$$\mathbf{y}_a(k)=\mathbf{C}_a\mathbf{x}_a(k), \tag{17}$$

where

$$\mathbf{C}_a=\begin{bmatrix}Q_1&0&\cdots&0\\0&Q_2&0&0\\0&0&\ddots&0\\0&0&0&Q_{N_a+1}\end{bmatrix},$$

$$Q_i=\begin{cases}1 & \text{when } \frac{N_a+1-i}{\ell} \text{ is an integer,}\\ 0 & \text{when } \frac{N_a+1-i}{\ell} \text{ is not an integer,}\end{cases}\qquad i=1,\ldots,N_a+1.$$

The augmented state vector and the measured output can be obtained as

$$\mathbf{x}_g(k)=\begin{bmatrix}\mathbf{x}(k)\\\mathbf{x}_a(k)\end{bmatrix},\quad \mathbf{y}_g(k)=\begin{bmatrix}\mathbf{y}(k)\\\mathbf{y}_a(k)\end{bmatrix}.$$

Then the augmented system, which includes the preview information, is

$$\begin{aligned}\mathbf{x}_g(k+1)&=\mathbf{A}_g\mathbf{x}_g(k)+\mathbf{B}_g\mathbf{u}(k)+\mathbf{D}_g\psi(k),\\ \mathbf{z}_1(k)&=\mathbf{C}_{g1}\mathbf{x}_g(k)+\mathbf{D}_{g1}\mathbf{u}(k),\\ \mathbf{z}_2(k)&=\mathbf{C}_{g2}\mathbf{x}_g(k)+\mathbf{D}_{g2}\mathbf{u}(k),\\ \mathbf{y}_g(k)&=\mathbf{C}_{gy}\mathbf{x}_g(k),\end{aligned} \tag{18}$$

where

$$\begin{aligned}\mathbf{F}&=\begin{bmatrix}\mathbf{F}_f&\mathbf{F}_r\end{bmatrix},\quad \mathbf{A}_g=\left[\begin{array}{c|ccc}\mathbf{G}&\mathbf{F}_r&\mathbf{0}_{8\times(N_a-1)}&\mathbf{F}_f\\\hline\mathbf{0}_{(N_a+1)\times 8}&\multicolumn{3}{c}{\mathbf{G}_a}\end{array}\right],\\ \mathbf{B}_g&=\begin{bmatrix}\mathbf{H}\\\mathbf{0}_{(N_a+1)\times 2}\end{bmatrix},\quad \mathbf{D}_g=\begin{bmatrix}\mathbf{0}_{8\times 1}\\\mathbf{F}_a\end{bmatrix},\\ \mathbf{D}_{w1}&=\begin{bmatrix}\mathbf{D}_{wf1}&\mathbf{D}_{wr1}\end{bmatrix},\quad \mathbf{C}_{g1}=\begin{bmatrix}\mathbf{C}_1&\mathbf{D}_{wr1}&\mathbf{0}_{2\times(N_a+1)}&\mathbf{D}_{wf1}\end{bmatrix},\\ \mathbf{D}_{w2}&=\begin{bmatrix}\mathbf{D}_{wf2}&\mathbf{D}_{wr2}\end{bmatrix},\quad \mathbf{C}_{g2}=\begin{bmatrix}\mathbf{C}_2&\mathbf{D}_{wr2}&\mathbf{0}_{6\times(N_a+1)}&\mathbf{D}_{wf2}\end{bmatrix},\\ \mathbf{D}_{gi}&=\mathbf{D}_i,\quad i=1,2.\end{aligned}$$

According to the different numbers of previewed data of the road disturbance used in the controller design, we define the following different conditions, and $\mathbf{C}_{gy}$ can be specified as

(1) *Active control without preview*:

$$\mathbf{C}_{gy}=\begin{bmatrix}\mathbf{C}_y&\mathbf{0}_{8\times(N_a+1)}\\\mathbf{0}_{(N_a+1)\times 8}&\mathbf{0}_{(N_a+1)\times(N_a+1)}\end{bmatrix}.$$

(2) *Active control with full-preview*: $T_p=T_s$.

$$\mathbf{C}_{gy}=\begin{bmatrix}\mathbf{C}_y&\mathbf{0}_{8\times(N_a+1)}\\\mathbf{0}_{(N_a+1)\times 8}&\mathbf{I}_{N_a+1}\end{bmatrix}.$$

(3) *Active control with partial-preview*: $T_p = \ell T_s$, $\ell = 2, 3, \ldots$.

$$\mathbf{C}_{gy} = \begin{bmatrix} \mathbf{C}_y & \mathbf{0}_{8\times(N_a+1)} \\ \mathbf{0}_{(N_a+1)\times 8} & \mathbf{C}_a \end{bmatrix}.$$

4. Multi-objective disturbance attenuation

The H_∞ and generalized H_2 norms of a transfer function operator $\mathbf{T}$ from $\overline{\mathbf{w}}$ to $\overline{\mathbf{z}}$ are defined, respectively, as

$$\|\mathbf{T}\|_\infty = \sup_{\overline{\mathbf{w}}\in l_2} \frac{\|\overline{\mathbf{z}}\|_2}{\|\overline{\mathbf{w}}\|_2},$$

$$\|\mathbf{T}\|_{GH_2} = \sup_{\overline{\mathbf{w}}\in l_2} \frac{\|\overline{\mathbf{z}}\|_\infty}{\|\overline{\mathbf{w}}\|_2}, \tag{19}$$

where

$$\|\overline{\mathbf{z}}\|_2 = \sqrt{\sum_{k=0}^{\infty} |\overline{\mathbf{z}}(k)|^2}, \quad \|\overline{\mathbf{w}}\|_2 = \sqrt{\sum_{k=0}^{\infty} |\overline{\mathbf{w}}(k)|^2}, \quad \|\overline{\mathbf{z}}\|_\infty = \sup_{k\in\mathbb{N}_0} |\overline{\mathbf{z}}(k)|.$$

Denote the transfer functions from disturbance ψ to the outputs $\mathbf{z}_1$ and $\mathbf{z}_2$ as $\mathbf{T}_1$ and $\mathbf{T}_2$, respectively. Then, the problem to be addressed in this paper is expressed as follows:

PF: Find a controller such that, with wheelbase preview, the augmented closed-loop system is internally stable, the H_∞ norm of $\mathbf{T}_1$ is minimized, and the generalized H_2 norm of $\mathbf{T}_2$ is less than a given γ_2.

Remark 1. The H_∞ norm and generalized H_2 norm should be used under energy-bounded disturbances, while a white-noise signal is an unbounded energy signal. In practice, since the excitation is studied over a finite-time span, the disturbance signal may be regarded as energy-bounded, hence it is suitable to use the H_∞ norm and the generalized H_2 norm as the indicators.

According to [39], the following lemmas are for the H_∞ and the generalized H_2 performance.

Lemma 1. *The system (18) with* $\mathbf{u} = \mathbf{0}$ *is asymptotically stable and* $\|\mathbf{T}_1\|_\infty < \gamma_1$ *if and only if there exists matrix* $\mathbf{P}_1 > \mathbf{0}$ *such that*

$$\begin{bmatrix} \mathbf{P}_1 & \mathbf{0} & \mathbf{A}_g\mathbf{P}_1 & \mathbf{D}_g \\ * & \gamma_1\mathbf{I} & \mathbf{C}_{g1}\mathbf{P}_1 & \mathbf{0} \\ * & * & \mathbf{P} & \mathbf{0} \\ * & * & * & \gamma_1\mathbf{I} \end{bmatrix} > \mathbf{0}. \tag{20}$$

Lemma 2. *The system (18) with* $\mathbf{u} = \mathbf{0}$ *is asymptotically stable and* $\|\mathbf{T}_2\|_{GH_2} < \gamma_2$ *if and only if there exists matrix* $\mathbf{P}_2 > \mathbf{0}$ *such that*

$$\begin{bmatrix} \mathbf{P}_2 & \mathbf{A}_g\mathbf{P}_2 & \mathbf{D}_g \\ * & \mathbf{P}_2 & \mathbf{0} \\ * & * & \mathbf{I} \end{bmatrix} > \mathbf{0}, \tag{21}$$

$$\begin{bmatrix} \gamma_2\mathbf{I} & \mathbf{C}_{g2}\mathbf{P}_2 \\ * & \mathbf{P}_2 \end{bmatrix} > \mathbf{0}. \tag{22}$$

Assume that a static output-feedback controller is used:

$$\mathbf{u}(k) = \mathbf{K}\mathbf{y}_g(k). \tag{23}$$

With this static output-feedback controller, we have the following proposition which can be obtained directly by considering Lemmas 1 and 2 together.

Proposition 1. *Closed-loop system (18) is asymptotically stable and satisfies* $\|\mathbf{T}_1\|_\infty < \gamma_1$, $\|\mathbf{T}_2\|_{GH_2} < \gamma_2$, *if there exist matrices* $\mathbf{P} > \mathbf{0}$ *and* $\mathbf{K}$ *such that*

$$\begin{bmatrix} \mathbf{P} & \mathbf{0} & (\mathbf{A}_g + \mathbf{B}_g\mathbf{K}\mathbf{C}_y)\mathbf{P} & \mathbf{D}_g \\ * & \gamma_1\mathbf{I} & (\mathbf{C}_{g1} + \mathbf{D}_{g1}\mathbf{K}\mathbf{C}_y)\mathbf{P} & \mathbf{0} \\ * & * & \mathbf{P} & \mathbf{0} \\ * & * & * & \gamma_1\mathbf{I} \end{bmatrix} > \mathbf{0}, \tag{24}$$

$$\begin{bmatrix} \mathbf{P} & (\mathbf{A}_g + \mathbf{B}_g\mathbf{K}\mathbf{C}_y)\mathbf{P} & \mathbf{D}_g \\ * & \mathbf{P} & \mathbf{0} \\ * & * & \mathbf{I} \end{bmatrix} > \mathbf{0}, \tag{25}$$

$$\begin{bmatrix} \gamma_2\mathbf{I} & (\mathbf{C}_{g2} + \mathbf{D}_{g2}\mathbf{K}\mathbf{C}_y)\mathbf{P} \\ * & \mathbf{P} \end{bmatrix} > \mathbf{0}. \tag{26}$$

The above matrix inequalities cannot be solved directly, because of the presence of some bilinear terms, such as $\mathbf{B}_g\mathbf{K}\mathbf{C}_y\mathbf{P}$. We employ the following ILMI iterations [45,46] to compute the output-feedback controller.

Algorithm ILMIs (Iterative Linear Matrix Inequalities):

1. Set $i=1$. Select the initial matrix $\mathbf{K}_1$ which is obtained from asymptotically stable condition that system (18) is asymptotically stable if and only if there exists a matrix $\mathbf{W} > \mathbf{0}$ and $\mathbf{K}_1$ such that
$$\begin{bmatrix} \mathbf{W} & \mathbf{A}_g + \mathbf{B}_g\mathbf{K}_1\mathbf{C}_y \\ * & \mathbf{W}^{-1} \end{bmatrix} > \mathbf{0}. \tag{27}$$
2. For fixed $\mathbf{K}_i$, solve the following optimization problem for $\mathbf{P}_i > \mathbf{0}$ and γ_{1i}.
OP: Minimize γ_{1i} subject to the following constraints
$$\begin{bmatrix} \mathbf{P}_i & \mathbf{0} & (\mathbf{A}_g + \mathbf{B}_g\mathbf{K}_i\mathbf{C}_y)\mathbf{P}_i & \mathbf{D}_g \\ * & \gamma_{1i}\mathbf{I} & (\mathbf{C}_{g1} + \mathbf{D}_{g1}\mathbf{K}_i\mathbf{C}_y)\mathbf{P}_i & \mathbf{0} \\ * & * & \mathbf{P}_i & \mathbf{0} \\ * & * & * & \gamma_{1i}\mathbf{I} \end{bmatrix} > \mathbf{0}, \tag{28}$$
$$\begin{bmatrix} \mathbf{P}_i & (\mathbf{A}_g + \mathbf{B}_g\mathbf{K}_i\mathbf{C}_y)\mathbf{P}_i & \mathbf{D}_g \\ * & \mathbf{P}_i & \mathbf{0} \\ * & * & \mathbf{I} \end{bmatrix} > \mathbf{0}, \tag{29}$$
$$\begin{bmatrix} \gamma_2\mathbf{I} & (\mathbf{C}_{g2} + \mathbf{D}_{g2}\mathbf{K}_i\mathbf{C}_y)\mathbf{P}_i \\ * & \mathbf{P}_i \end{bmatrix} > \mathbf{0}. \tag{30}$$
3. For fixed $\mathbf{P}_i > \mathbf{0}$, solve the following feasibility problem for $\mathbf{K}_i$.
FP: Find $\mathbf{K}_i$ subject to LMIs (28)–(30)
4. If $|(\gamma_i - \gamma_{i-1})| < \varepsilon$, where $\varepsilon > 0$ is a prescribed tolerance, then STOP.
else set $i = i+1$ and $\mathbf{K}_i = \mathbf{K}_{i-1}$, then go to Step 2.

The asymptotic stability condition in (27) cannot be solved directly by using convex programming techniques, a cone complementarity linearization (CCL) algorithm [47–49] is proposed here, and we introduce a new matrix $\mathbf{Q} > \mathbf{0}$. Then inequality (27) holds if

$$\begin{bmatrix} \mathbf{W} & \mathbf{A}_g + \mathbf{B}_g\mathbf{K}\mathbf{C}_y \\ * & \mathbf{Q} \end{bmatrix} > \mathbf{0}, \tag{31}$$

$$\begin{bmatrix} \mathbf{W} & \mathbf{I} \\ * & \mathbf{Q} \end{bmatrix} \geq \mathbf{0}, \tag{32}$$

$$\mathbf{W}\mathbf{Q} = \mathbf{I}. \tag{33}$$

According to the above LMIs, the CCL algorithm can be formulated in the following algorithm.

Algorithm CCL (*cone complementarity linearization*):

1. Set $i=1$. Choosing initial $\mathbf{W}_0>\mathbf{0},\mathbf{Q}_0>\mathbf{0}$ randomly.
2. Solve

$$\begin{aligned}&\min \operatorname{tr}(\mathbf{W}^i\mathbf{Q}+\mathbf{W}\mathbf{Q}^i)\\&\text{subject to (31) and (32).}\end{aligned}$$

   Set $\mathbf{W}^i=\mathbf{W},\mathbf{Q}^i=\mathbf{Q}$.
3. Substitute the obtained matrix $\mathbf{W}$ into (27). If one of the inequalities (27) and

$$|\operatorname{tr}(\mathbf{W}^i\mathbf{Q}+\mathbf{W}\mathbf{Q}^i)-2n|<\rho,\quad n=\dim(\mathbf{A}_g). \tag{34}$$

   is not satisfied with some sufficiently small $\rho>0$, then set $i=i+1$ and go to Step 2. Otherwise, EXIT.

5. Simulation results

In this section, the results of multi-objective control with wheelbase preview for a half-car model are studied. The performances of vehicle suspension with passive control, multi-objective control with full-preview, partial-preview and without preview are compared. It is assumed that the preview information is obtained from system responses under the front wheel disturbance. The vehicle parameters for a compact sedan [6] used in simulation are listed in Table 1, and choosing $z_{f\max}=z_{r\max}=0.08$ m, $u_{f\max}=u_{r\max}=1000$ N. The parameters of road roughness are chosen as $\alpha=0.45\ \mathrm{m}^{-1}$, $\sigma^2=300\times10^{-6}\ \mathrm{m}^2$.

The vehicle is assumed to run linearly with a constant velocity of 20 m/s, and the system sampling period is $T_s=0.025$ s. Since the natural frequencies of the heave mode and pitch mode of this system are less than 20 Hz, this sampling period is sufficient to capture the essential vibration characteristics.

According to the above parameters, $N_a=5$. Combining with $w_f(k)$, there are at most six preview data for the rear wheel. Considering the preview sampling period T_p, when $\ell>6$, the available preview information is the same after preview sampling, that is, $\mathbf{C}_a$ is the same, so we choose $\ell=1,\ldots,6$, for comparing the performances of different conditions of control

Table 1
Model parameters.

M	J	m_f	m_r
500 kg	910 kg m^2	30 kg	40 kg
$k_{f\,1}$	$k_{r\,1}$	$k_{f\,2}$	$k_{r\,2}$
10,000 N/m	10,000 N/m	100,000 N/m	100,000 N/m
b_f	b_r	a	b
1000 N s/m	1000 N s/m	1.25 m	1.45 m

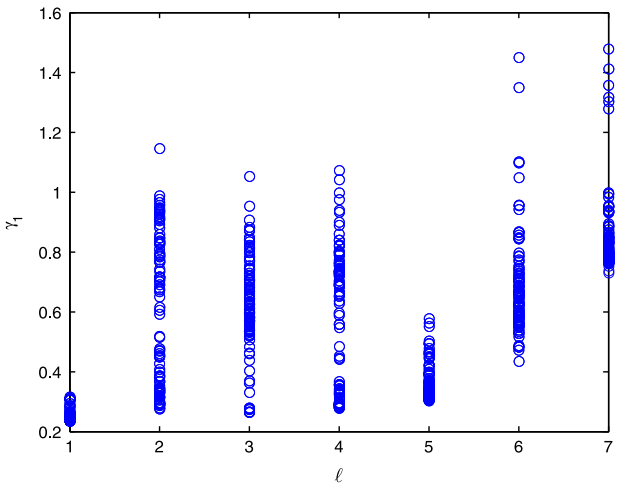

Fig. 2. γ_1 comparison.

with preview. The condition $\ell=1$ corresponds to active control with full-preview, the condition $\ell=6$ corresponds to preview information only including $w_f(k)$. Let us define $\ell=7$ as the condition that multi-objective control without preview in subsequent discussions.

Since different initial conditions of $\mathbf{K}_1$ used in Algorithm ILMIs will result in different controllers, hundreds of runs with different initial conditions are tested. The minimum γ_1 and the corresponding $\mathbf{K}$ of each case are used in the comparison. Fig. 2 shows the γ_1 of different cases. Table 2 lists the minimum value of each condition. It can be seen that γ_1 of control with preview ($\ell=1,\ldots,6$) are significantly less than that of control without preview ($\ell=7$). As for different conditions of control with preview, the more preview information, the smaller γ_1 we get, that is, γ_1 of $\ell=1$ is the smallest one, γ_1 of $\ell=2$ is smaller than that of $\ell=4$, and γ_1 for all of $\ell=1,2,\ldots,5$ are smaller than that of $\ell=6$.

Figs. 3 and 4 show the vehicle vertical (heave mode) and angular (pitch mode) accelerations for different conditions separately. Fig. 3 compares the responses of passive control, multi-objective control without preview, multi-objective with full-preview ($\ell=1$). As expected, both the vertical and angular accelerations of control with preview, especially the angular acceleration, are lower than that of control without preview. This indicates that active suspension with preview can provide better ride quality. Fig. 4 shows the response of multi-objective control with different numbers of preview information, accelerations of control with full-preview ($\ell=1$) and with partial-preview ($\ell=6$) are chosen to compare. The difference

Table 2
Minimal γ_1 under different conditions.

ℓ	1	2	3	4	5	6	7
γ_1	0.2342	0.2752	0.2640	0.2778	0.3025	0.4346	0.7601

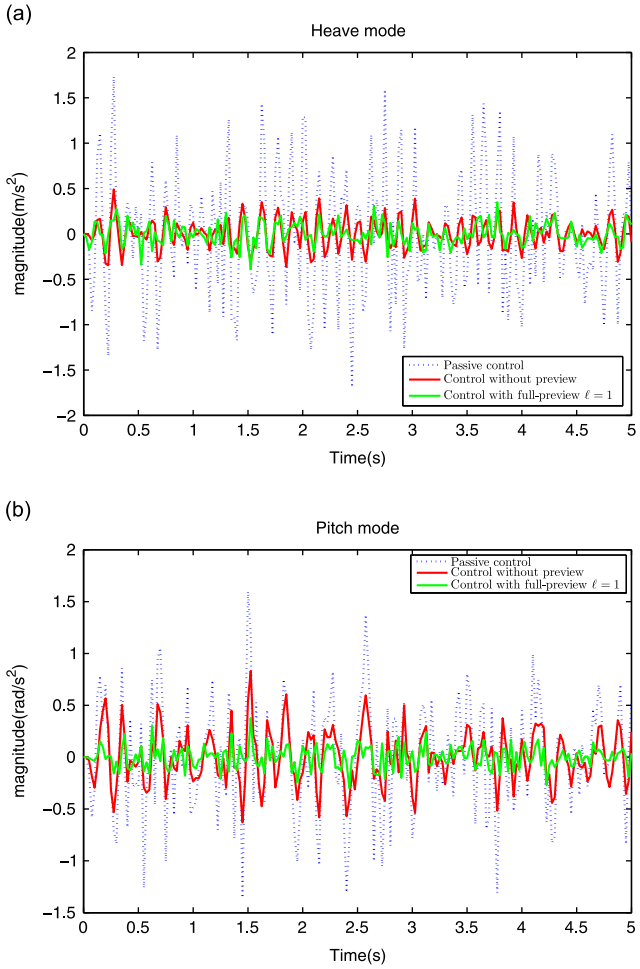

Fig. 3. Response comparison of passive control, active control with and without preview. (a) Vertical acceleration comparison; (b) angular acceleration comparison.

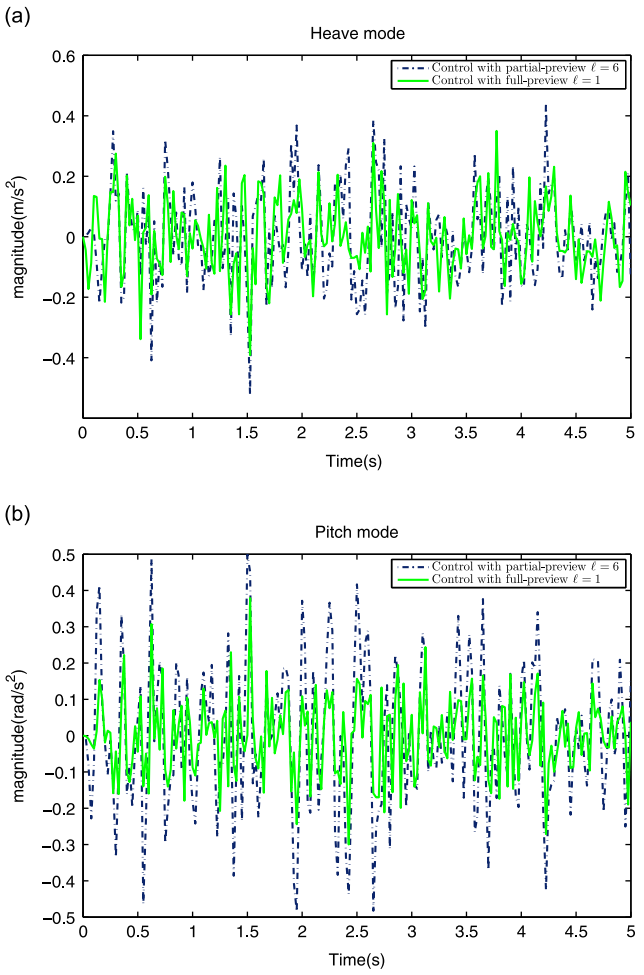

Fig. 4. Response comparison of active control with different numbers of preview information. (a) Vertical acceleration comparison; (b) angular acceleration comparison.

between vertical acceleration is slight, but the angular acceleration of control with full-preview is obviously less than that of control with partial-preview.

To assess the performance of the vibration reduction in the heave and pitch modes, we provide the root mean square (RMS) values of the signals $\ddot{z}_c$ and $\ddot{\theta}$ of different conditions. Denote T_θ as the transfer function from ψ to $\ddot{\theta}$, then the RMS value of $\ddot{\theta}$ and H_2 norm of T_θ can be given by

$$\|\ddot{\theta}\|_{\mathrm{rms}} = \sqrt{\left(\frac{1}{2\pi}\int_{-\pi}^{\pi} |T_\theta(e^{j\omega})|^2 S_\psi(\omega)\,\mathrm{d}\omega\right)}$$

$$\|T_\theta\|_2 = \sqrt{\left(\frac{1}{2\pi}\int_{-\pi}^{\pi} |T_\theta(e^{j\omega})|^2\right)\mathrm{d}\omega)}$$

where S_ψ is the Power Spectral Density of disturbance ψ. Since ψ is white noise input, $S_\psi(\omega)=1$, the RMS value equals the H_2 norm. In this way, RMS value of $\ddot{z}_c$ and $\ddot{\theta}$ based on the H_2 norm of their respective transfer function is used to compare. The RMS value of $\ddot{z}_c, \ddot{\theta}$ under four different conditions is listed in Table 3. It can be clearly seen that active control with partial-preview reduces the vertical acceleration of control without preview by up to 19 percent, control with full-preview further reduces the acceleration of control with partial-preview up to 10 percent. As for angular acceleration, control with partial-preview provides 25 percent improvement comparing with that of control without preview, while control with full-preview provides 46 percent more improvement than that of control with partial-preview. In general, comparing with control without preview, both vertical and angular accelerations are attenuated by control with preview, and angular acceleration is attenuated more significant than vertical acceleration.

Fig. 5 compares $\|\mathbf{T}_1(e^{j\omega})\|$ of vehicle suspension with passive control, active control without preview and with full-preview ($\ell=1$) for $0<\omega<\pi$. The heave mode and pitch mode correspond to the first peak and second peak, respectively.

Table 3
RMS $\ddot{z}_c, \ddot{\theta}$ under different conditions.

Signal	Control			
	Passive	Multi-objective	With preview ($\ell=6$)	With preview ($\ell=1$)
RMS $\ddot{z}_c$	0.7572	0.1923	0.1564	0.1417
RMS $\ddot{\theta}$	0.5502	0.2722	0.2050	0.1104

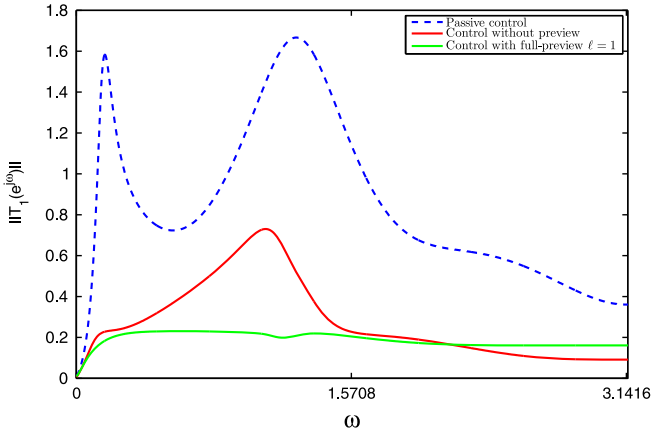

Fig. 5. Frequency responses comparison.

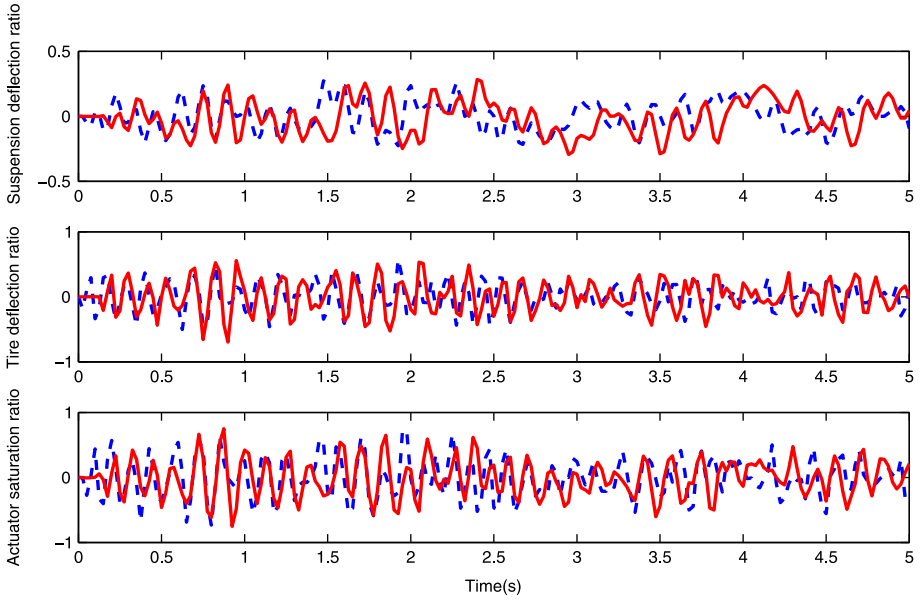

Fig. 6. $\mathbf{z}_2$ responses comparison. - - - -, responses of front assemblies; ——, responses of rear assemblies.

The highest peak value equals $\|\mathbf{T}_1\|_\infty$ in each situation. It can be seen that both heave mode and pitch mode peak values have been reduced by control without preview, especially the frequency response of heave mode is almost flat. That explains why the vertical acceleration is only reduced slightly by control with preview when compared to control without preview. The figure also shows under control with full-preview, the peak value of the pitch mode has also been significantly attenuated, which illustrates that control with full-preview can provide better ride quality than control without preview.

Fig. 6 shows the active suspension disturbance responses of $\mathbf{z}_2$ under control with full-preview, the dashed lines denote the responses of the front assemblies, the responses of rear assemblies are shown by the solid lines. It can be seen that the suspension deflection, tyre deflection and actuator saturation are all having absolute values strictly less than unity (that is, they all do not violate the physical constraints).

6. Conclusions

Based on the wheelbase preview method, a multi-objective control method for vehicle suspension has been proposed. H_∞ norm is used as the indicator of ride quality, and generalized H_2 norm is utilized to constrain suspension deflection, tyre deflection and actuator saturation. Algorithms ILMIs and CCL are used to derive the control gain of static output-feedback. The performances of vehicle suspension under different conditions are compared. The results illustrate that the proposed control method achieves better performance than that of control without preview, and further improvement can be obtained with more preview information. The application of active control is important for high-performance vehicles but at the expense of higher power usage. It is generally recognized that this has limited its use in common vehicle systems.

Acknowledgments

The work is partially supported by HKU CRCG 201109176086 and HKU CRCG 201109176085.

References

[1] R. Rajamani, *Vehicle Dynamics and Control*, Springer, New York, 2012.
[2] E. Bender, Optimum linear preview control with application to vehicle suspension, *Journal of Basic Engineering* 90 (2) (1968) 213–221.
[3] M. Tomizuka, Optimal continuous finite preview problem, *IEEE Transactions on Automatic Control* 21 (3) (1975) 362–365.
[4] A. Hac, Optimal linear preview control of active vehicle suspension, *Vehicle System Dynamics* 21 (1) (1992) 167–195.
[5] J. Marzbanrad, Y. Hojjat, H. Zohoor, S. Nikravesh, Optimal preview control design of an active suspension based on a full car model, *Scientia Iranica* 10 (1) (2003) 23–26.
[6] J. Marzbanrad, G. Ahmadi, H. Zohoor, Y. Hojjat, Stochastic optimal preview control of a vehicle suspension, *Journal of Sound and Vibration* 275 (3–5) (2004) 973–990.
[7] H. Roh, Y. Park, Stochastic optimal preview control of an active vehicle suspension, *Journal of Sound and Vibration* 220 (2) (1999) 313–330.
[8] A.G. Thompson, C.E. Pearce, Direct computation of the performance index for an optimally controlled active suspension with preview applied to a half-car model, *Vehicle Systems Dynamics* 35 (2) (2001) 121–137.
[9] A. Vahidi, A. Eskandarian, Influence of preview uncertainties in the preview control of vehicle suspensions, *Proceedings of the Institution of Mechanical Engineers Part K: Journal of Multi-body Dynamics* 216 (4) (2002) 295–301.
[10] M. Elmadany, Z. Abduljabbar, M. Foda, Optimal preview control of active suspensions with integral constraint, *Journal of Vibration and Control* 9 (12) (2003) 1377–1400.
[11] A.G. Thompson, B.R. Davis, Computation of the RMS state variable and control forces in a half-car model with preview active suspension using spectral decomposition methods, *Journal of Sound and Vibration* 285 (3) (2005) 571–583.
[12] I. Youn, A. Hac, Preview control of active suspension with integral action, *International Journal of Automotive Technology* 7 (5) (2006) 547–554.
[13] L.V.V. Rao, S. Narayanan, Preview control of random response of a half car vehicle model traversing a rough road, *Journal of Sound and Vibration* 310 (1–2) (2008) 352–365.
[14] R.S. Prabakar, C. Sujatha, S. Narayanan, Optimal semi-active preview control response of a half car vehicle model with magnetorheological damper, *Journal of Sound and Vibration* 326 (3–5) (2009) 400–420.
[15] F. Yu, D. Crolla, Wheelbase preview optimal control for active vehicle suspensions, *Chinese Journal of Mechanical Engineering* 2 (1998) 122–130.
[16] F. Yu, J. Zhang, D. Crolla, A study of a Kalman filter active vehicle suspension system using correlation of front and rear wheel road inputs, *Proceedings of the Institution of Mechanical Engineers, Part D: Journal of Automobile Engineering* 214 (5) (2000) 493–502.
[17] Y. Park, H. Roh, Observer-based wheelbase preview control of active vehicle suspensions, *KSEME International Journal* 12 (5) (1998) 782–791.
[18] Z. Xie, P. Wong, X. Huang, H. Wong, Design of an active vehicle suspension based on an enhanced PID control with wheelbase preview and tuning using genetic algorithm, *Journal of the Chinese Society of Mechanical Engineers* 33 (2012) 103–112.
[19] X. Zhang, J. Zhang, Performance analysis of limited bandwidth active suspension with preview based on a discrete time model, *WSEAS Transactions on Systems* 9 (8) (2010) 834–843.
[20] K.S. Hong, H. Sohn, J. Hedrick, Modified skyhook control of semi-active suspensions: *a new model, gain scheduling and hardware-in-the-loop tuning, Journal of Dynamic Systems, Measurement, and Control* 124 (2002) 158–167.
[21] M. Zapateiro, F. Pozo, H. Karimi, Semi-active control methodologies for suspension control with magnetorheological dampers, *IEEE-ASME Transactions on Mechatronics* 17 (2) (2012) 370–380.
[22] H. Du, W. Li, N. Zhang, Semi-active variable stiffness vibration control of vehicle seat suspension using an MR elastomer isolator, *Smart Materials and Structures* 20 (2011) 10.
[23] J.H. Crews, M.G. Mattson, G.D. Buckner, Multi-objective control optimization for semi-active vehicle suspensions, *Journal of Sound and Vibration* 330 (23) (2011) 5502–5516.
[24] J. Tudon-Martinez, S. Fergani, S. Verrier, O. Sename, L. Dugard, R. Morales-Menendez, R.A. Ramirez-Mendoza, Road adaptive semi-active suspension in an automotive vehicle using an LPV controller, *Advances in Automotive Control* 7 (2013) 231–236.
[25] H. Chen, C. Long, C. Yuan, H. Jiang, Non-linear modelling and control of semi-active suspensions with variable damping, *Vehicle System Dynamics* 51 (10) (2013) 1568–1587.
[26] H. Du, N. Zhang, Fuzzy control for nonlinear uncertain electrohydraulic active suspension with input constraint, *IEEE Transactions on Fuzzy Systems* 17 (2) (2009) 343–356.
[27] H. Du, N. Zhang, Takagi–Sugeno fuzzy control scheme for electrohydraulic active suspensions, *Control and Cybernetics* 39 (4) (2010) 1095–1115.
[28] H. Li, H. Liu, H. Gao, P. Shi, Reliable fuzzy control for active suspension systems with actuator delay and fault, *IEEE Transactions on Fuzzy Systems* 20 (2) (2012) 342–357.
[29] H. Du, N. Zhang, F. Naghdy, Robust control of vehicle electrorheological suspension subject to measurement noises, *Vehicle System Dynamics* 49 (1–2) (2011) 257–275.
[30] W. Sun, H. Gao, O. Kaynak, Saturated adaptive robust control for active suspension systems, *IEEE Transactions on Industrial Electronics* 60 (9) (2013) 3889–3896.
[31] H. Li, X. Jing, H.R. Karimi, Output-feedback-based H_∞ control for vehicle suspension systems with control delay, *IEEE Transactions on Industrial Electronics* 61 (1) (2014) 436–446.
[32] W. Sun, H. Gao, B. Yao, Adaptive robust vibration control of full-car active suspensions with electrohydraulic actuators, *IEEE Transactions on Control Systems Technology* 21 (6) (2013) 2417–2422.
[33] G. Koch, T. Kloiber, Driving state adaptive control of an active vehicle suspension system, *IEEE Transactions on Control Systems Technology* 22 (1) (2014) 44–57.

[34] W. Sun, H. Gao, O. Kaynak, Finite frequency H_∞ control for vehicle active suspension systems, *IEEE Transactions on Control Systems Technology* 19 (2) (2011) 416–422.
[35] H. Chen, P. Sun, K. Guo, A multi-objective control design for active suspensions with hard constraints, *Proceedings of the American Control Conference* 1 (2003) 4371–4376.
[36] H. Gao, J. Lam, C. Wang, Multi-objective control of vehicle active suspension systems via load-dependent controllers, *Journal of Sound and Vibration* 290 (3–5) (2006) 654–675.
[37] M. Gobbi, F. Levi, G. Mastinu, Multi-objective stochastic optimization of the suspension system of road vehicles, *Journal of Sound and Vibration* 298 (4–5) (2006) 1055–1072.
[38] A. Akbari, G. Koch, E. Pellegrini, B. Lohmann, Multi-objective preview control of active vehicle suspensions: *experimental results*, *Advanced Computer Control* 3 (2010) 497–502.
[39] A. Akbari, B. Lohmann, Output feedback H_∞/GH_2 preview control of active vehicle suspensions: *a comparison study of LQG preview*, *Vehicle System Dynamics* 48 (12) (2010) 1475–1494.
[40] T. Gordon, C. Marsh, M. Milsted, A comparison of adaptive LQG and nonlinear controllers for vehicle suspension system, *Vehicle System Dynamics* 20 (6) (1991) 321–340.
[41] J. Marzbanrad, G. Ahmadi, Y. Hojjat, H. Zohoor, Optimal active control of vehicle suspension system including time delay and preview for rough roads, *International Journal of Control* 8 (7) (2002) 967–991.
[42] A. Gonzalez, E. OBrien, Y. Li, K. Cashell, The use of vehicle acceleration measurement to estimate road roughness, *Vehicle System Dynamics* 46 (6) (2008) 483–499.
[43] H. Singer, A survey of estimation methods for stochastic differential equations, *Proceedings of 6th International Conference on Social Science Methodology*, 2004.
[44] X. Mao, *Stochastic Differential Equations and Their Applications*, Horwood, New York, 1997.
[45] Y. Cao, J. Lam, Y. Sun, Static output feedback stabilization: *an ILMI approach*, *Automatica* 34 (12) (1998) 1641–1645.
[46] X. Chen, J. Lam, P. Li, Z. Shu, ℓ_1-induced norm and controller synthesis of positive systems, *Automatica* 49 (5) (2013) 1377–1385.
[47] H. Gao, C. Wang, Comments and further results on 'a descriptor system approach to H_∞ control of linear time-delay systems', *IEEE Transactions on Automatic Control* 48 (2003) 520–525.
[48] B. Zhang, S. Zhou, S. Xu, Delay-dependent H_∞ controller design for linear neutral systems with discrete and distributed delays, *International Journal of Systems Science* 38 (8) (2007) 611–621.
[49] B. Zhang, G. Tang, Active vibration H_∞ control of offshore steel jacket platforms using delayed feedback, *Journal of Sound and Vibration* 332 (22) (2013) 5662–5677.